The Adaptive PLIC-VOF Method with Overset Meshes

MARINE 2021

Dezhi Dai[1,*] and Albert Y. Tong[2]

[1] Nuclear Science and Engineering Division, Argonne National Laboratory, Lemont, IL 60439, USA, Email: daid@anl.gov, Web page: https://www.anl.gov/

[2] Mechanical and Aerospace Engineering Department, University of Texas at Arlington, Arlington, TX 76019, USA, Email: tong@uta.edu, Web page: https://www.uta.edu/

[*] Corresponding author: Dezhi Dai, daid@anl.gov

ABSTRACT

Piecewise Linear Interface Calculation (PLIC) schemes have been extensively employed in the Volume of Fluid (VOF) method to capture the interface between water and air in marine applications. The Adaptive Mesh Refinement (AMR) is often adopted to increase the local mesh resolution dynamically within the cells which are close to or contain the interface. Dynamic overset meshes can be especially useful in applications involving component motions involving ship/offshore platform hydrodynamics, semi-submerged propellers, water entry/exiting, etc. An adaptive PLIC-VOF method with overset mesh for static objects has been introduced in the present study. Simulations are performed under the framework of OpenFOAM with a modified flow solver. Numerical simulations of two dam-breaking problems with overset meshes and adaptive PLIC-VOF method have been successfully performed. An extension of solid body movement supporting is currently ongoing.

Keywords: VOF; PLIC; Overset; AMR; OpenFOAM; multi-phase flows.

NOMENCLATURE

α	Liquid volume fraction [-]
$\vec{U}$	Velocity field [m s^{-1},m s^{-1},m s^{-1}]
t	time [s]
Δt	Time step [s]
Ω_P	Volume of CV P [m^3]
N_f	Face numbers of CV P [-]
$\vec{S}_f$	Outward area vector of face f [m^2,m^2,m^2]
ϕ_f^t	Volumetric flux across face f at t [m^3 s^{-1}]
$A_f(t)$	Submerged area on face f [m^2]
ΔV_f	Liquid volume transported across face f during the time interval [m^3]
$\vec{n}$	Unit outward normal vector of the interface [-,-,-]
$\vec{X}$	Position vector of the interface [m,m,m]
D	Signed distance from the origin [m]
ϵ_l	Lower *alpha* limitation in mesh refinement [-]
ϵ_u	Upper *alpha* limitation in mesh refinement [-]
PLIC	Piecewise Linear Interface Calculation
VOF	Volume of Fluid
AMR	Adaptive Mesh Refinemen

1 INTRODUCTION

The water-air two-phase flows are common scenarios in marine applications. The Volume of Fluid (VOF) method is widely used in capturing the interface between different immiscible phases. The VOF method introduces a scalar variable called the VOF function α, which is defined as the liquid volume fraction in a computational cell with zero for gas phase, unity for liquid phase, and between zero and one for mixed (interface) cells, respectively. The Piecewise Linear Interface Calculation (PLIC) schemes (Roenby et al., 2016, Dai and Tong, 2018, 2019) have been extensively employed in the VOF equation solving to keep the interface sharp while maintaining mass conservation at the expense of an extra reconstruction step.

However, high mesh resolution is still essential to resolve the interface between liquid and gas phases in a VOF simulation by using the PLIC-VOF method. The Adaptive Mesh Refinement (AMR) method (Rettenmaier et al., 2019) is usually adopted to refine the mesh density dynamically by splitting the cells into several child cells near the interface of the two-phase flows. Meanwhile, the α field mapping between the refined and unrefined meshes is critical in the adaptive PLIC-VOF method. In the *dynamicRefineFvMesh* library from *OpenFOAM-v2006*, the mapping scheme is implemented algebraically. The default algebraic field mapping from the parent cell to child ones is mass conservative, but has not taken the interface orientation into consideration, which will break the consistent property of the interface in the parent cell. A geometric interpolation scheme has been developed in (Scheufler and Roenby, 2019) and its source code is available in (Scheufler). It should be noted that the implementation in (Scheufler) has been improved in the present study. In (Scheufler), the geometric intersections between the interface planes and candidate cells will be applied to all of the mixed cells, whereas the same operation will be performed only on the child cells from the mesh refinement at the current time step, which improved the computational efficiency.

The dynamic overset meshes can be especially useful in marine applications involving component motions involving ship/offshore platform hydrodynamics, semi-submerged propellers, water entry/exiting, etc. The computational domain is discretized with multiple disconnected meshes. The background mesh represents the whole domain which is usually static, and the body ones cover partial domain around the moving/stationary objects of interest. The flow fields in different mesh regions are synced by using overset interpolations at each time step. A detailed description of the overset approach and interpolation schemes is available in (Chang et al., 2020).

The adaptive PLIC-VOF method has been extended to overset meshes with static bodies in the present study. An extension of solid body movements is currently ongoing. Two dam-breaking problems with fixed obstacles have been employed to verify the methods introduced by the present study. A brief overview of the numerical formulations is presented next followed by the simulation results.

2 NUMERICAL FORMULATIONS

2.1 VOF Equation Solving

The fraction field is transportated by:

$$\frac{\partial \alpha}{\partial t} + \nabla \cdot \left(\alpha \vec{U}\right) = 0, \tag{1}$$

where t and $\vec{U}$ are the time and velocity field, respectively.

Integrating the VOF equation (Eq. (1)) over the control volume (CV) P from t to $t + \Delta t$ gives

$$\int_t^{t+\Delta t} \left(\int_{\Omega_P} \frac{\partial \alpha}{\partial t} \, d\Omega \right) dt + \int_t^{t+\Delta t} \left(\int_{\Omega_P} \nabla \cdot (\alpha U) \, d\Omega \right) dt = 0, \tag{2}$$

where Ω_P is the volume of CV P. Then the updated volume fraction is given by:

$$\alpha_P^{t+\Delta t} = 1 - \frac{1}{\Omega_P} \sum_{f=1}^{N_f} \underbrace{\left(\frac{\phi_f^t}{\left|\vec{S}_f\right|} \int_t^{t+\Delta t} A_f(t)\, dt \right)}_{\Delta V_f}, \tag{3}$$

where N_f is the face numbers of CV P, $\vec{S}_f$ the outward area vector of face f, $\phi_f^t \left(= U_f^t \cdot \vec{S}_f\right)$ the volumetric flux across face f at t and $A_f(t) \left(= \alpha_f(t) \left|\vec{S}_f\right|\right)$ the submerged area on face f. The term ΔV_f represents the liquid volume transported across face f during the time interval.

In the PLIC-VOF method, the face submerged area $A_f(t)$ is calculated by using an approximated interface plane inside its upwind adjacent cell, from which this face receives fluid during the time step (Roenby et al., 2016). As shown in Figure 1, the interface is approximated as a plane in a mixed cell, and its can be expressed as

$$\vec{n} \cdot \vec{X} + D = 0, \tag{4}$$

where $\vec{n}$ is the unit outward normal vector of the interface, $\vec{X}$ the position vector of the interface, and D the signed distance from the origin. In the present project, the $\vec{n}$ is evaluated by using the fraction gradient, i.e.,

$$\vec{n} = -\frac{\nabla \alpha}{\|\nabla \alpha\|} \tag{5}$$

where the negative sign indicates that the vector $\vec{n}$ points from liquid to gas. Once the orientation vector $\vec{n}$ has been determined, the signed distance D is calculated by the Optimized-SEC scheme developed in (Dai and Tong, 2019). Finally, the face submerged area $A_f(t)$ is evaluated following the method in (Roenby et al., 2016).

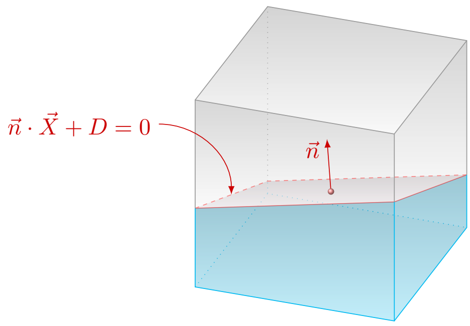

Figure 1: Approximated interface inside a mixed cell.

2.2 Adaptive PLIC-VOF Method

In the AMR method, a hexahedral cell is refined by splitting it into eight child cells. In the present study, the fraction value is adopted to trigger the mesh refinement and coarsening. Two limitation values, ϵ_l and ϵ_u, are specified. Any cells with fraction values between ϵ_l and ϵ_u will be refined up to a predefined maximum refinement level, and the others will be coarsened. The values of ϵ_l and ϵ_u are set to 0.001 and 0.999, respectively.

In OpenFOAM, the child cells take the value of their parent cell directly in a cell refinement process, i.e.,

$$\alpha_c = \alpha_p, \tag{6}$$

and a volume-averaged fraction value of the child cells will be set to the parent one in a cell coarsening step, i.e.,

$$\alpha_p = \frac{\sum_{i=1}^{8} \alpha_{c,i} \Omega_{c,i}}{\sum_{i=1}^{8} \Omega_{c,i}}. \tag{7}$$

As stated in (Scheufler and Roenby, 2019), the reconstructed interface in the parent cell has been employed to cut its child cells, then their fraction values are the volume ratios between the submerged parts and them (see Figure 2). Similar with (Chang et al., 2020), the fraction value of a child cell is given by:

$$\alpha_c = \frac{\Omega_{sub}}{\Omega_c}, \tag{8}$$

where Ω_{sub} represents the submerged parts (see Figure 2, marked in blue) of the child cell truncation by the interface plane in its parent cell.

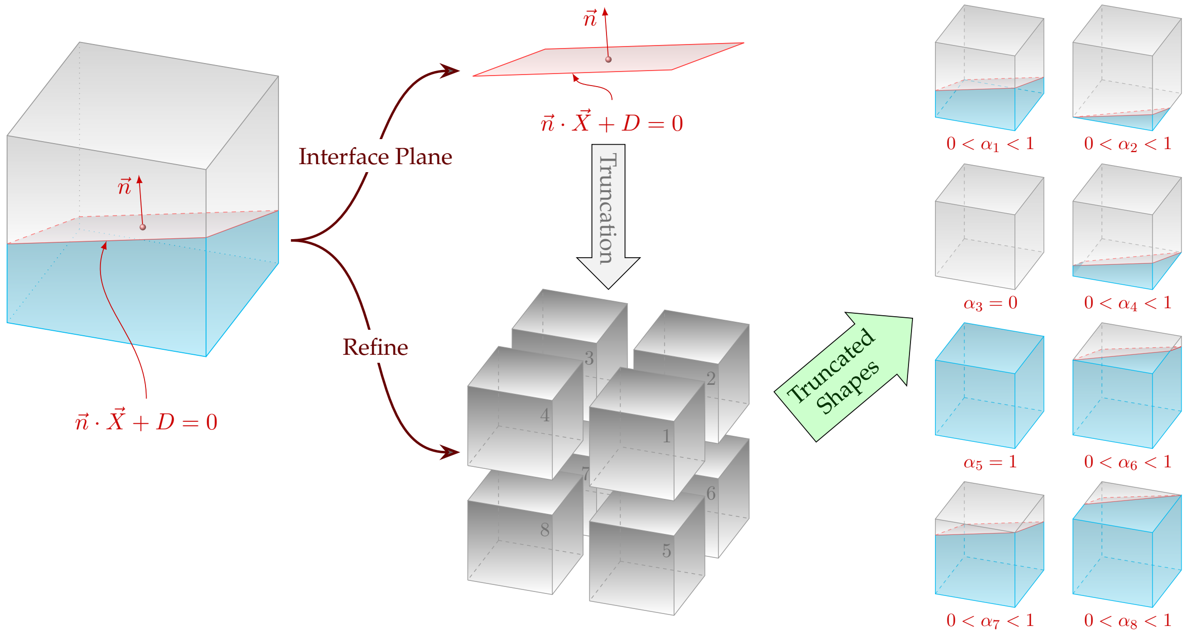

Figure 2: Illustration of the geometric fraction field mapping.

2.3 Adaptive PLIC-VOF Method with Overset Meshes

The implementation of the adaptive PLIC-VOF method with overset meshes is based on the *dynamicRefineFvMesh* and *dynamicOversetFvMesh* libraries in *OpenFOAM-v2006*. During each time step, the solving procedures are following:

1. Refine/coarsen the computational cells based on the criteria $\epsilon_l \leq \alpha \leq \epsilon_u$.
2. Interpolate flow fields by using Eqs. (6) and (7).
3. Interpolate the α field in child cells only by using Eq. (8).
4. Detect cell types in different mesh regions.
5. Interpolate the flow fields between the background and body meshes.
6. Inner iteration:
   - Solve the VOF equation (Eq. (1)) by using the PLIC-VOF method.
   - Solve the velocity and pressure fields.

3 SIMULATION RESULTS

To examine the performance of the adaptive PLIC-VOF method with overset meshes, the 2D and 3D dam-breaking problems, which are typical test cases for gravitational force-dominant water-air two-phase flows are considered. As shown in Figure 3a, a $0.1461\,m \times 0.292\,m$ water column is placed on the left wall of a square tank with a side length of $0.584\,m$ initially, and the dam-breaking phenomenon occurs under the action of gravity. A $0.024\,m \times 0.048\,m$ obstacle is placed $0.032\,m$ above the tank bottom surface. A wave probe at $y = 0.16\,m$ is used to track the time history of water heights.

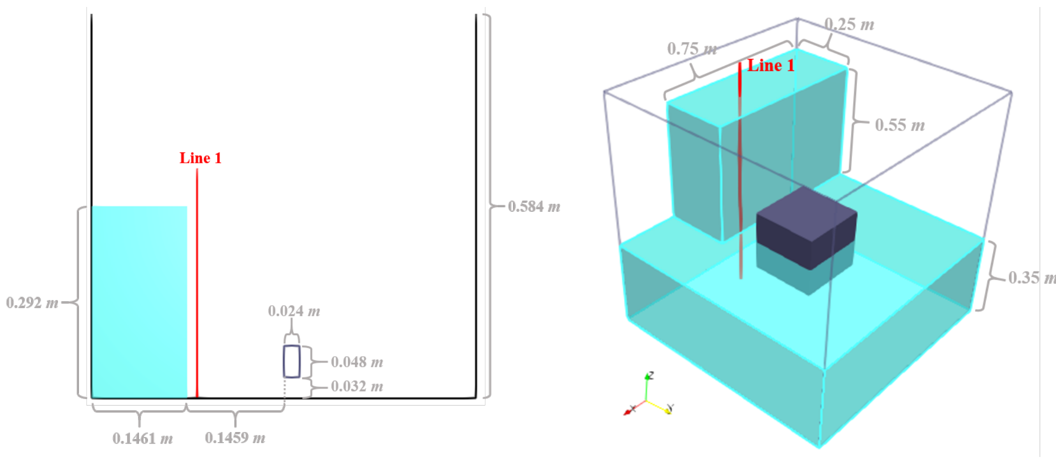

(a) 2D dam-breaking (b) 3D dam-breaking

Figure 3: Configurations of the dam-breaking problems.

The 3D dam-breaking case configuration is shown in Figure 3b, a composite water column shape is placed in a unit cubic tank. A cube box with a side length of $0.25\,m$ is placed $0.1\,m$ above the tank bottom surface. Same as the 2D case, a wave probe at $x = 0.5$ and $y = 0.15\,m$ is used to track the time history of water heights.

The meshes used in the 2D and 3D dam-breaking problems are shown in Figure 4. The meshes in blue and red represent the background and body meshes, respectively.

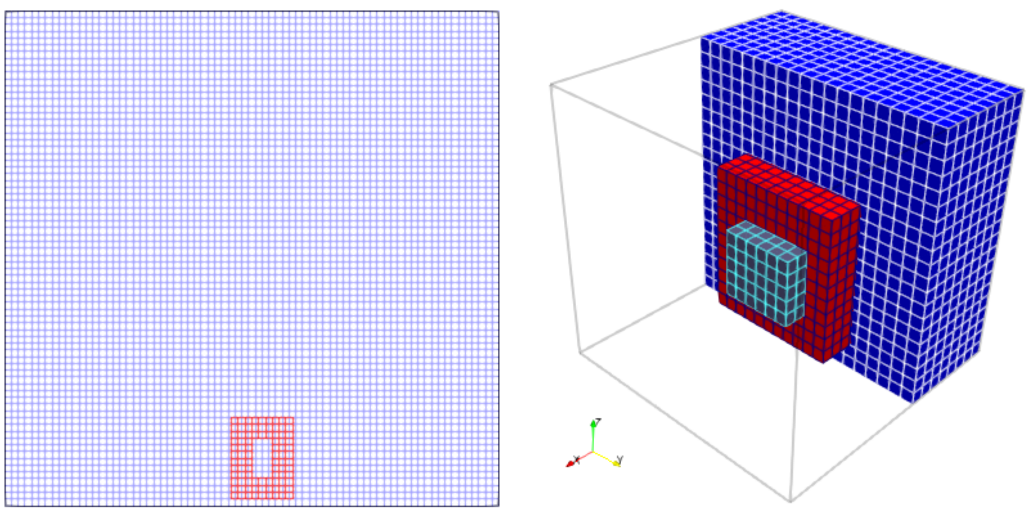

(a) 2D dam-breaking (b) 3D dam-breaking

Figure 4: Overset meshes of the dam-breaking problems.

3.1 2D Dam-breaking Simulation

The fraction field distributions with different AMR levels at various time instants are shown in Figure 5. It is clearly shown that the interface has been better resolved, and smaller droplets have been captured with increasing AMR levels. As shown in Figure 6, the transient water heights at the pre-defined probe have been found to be convergent as the AMR level increases.

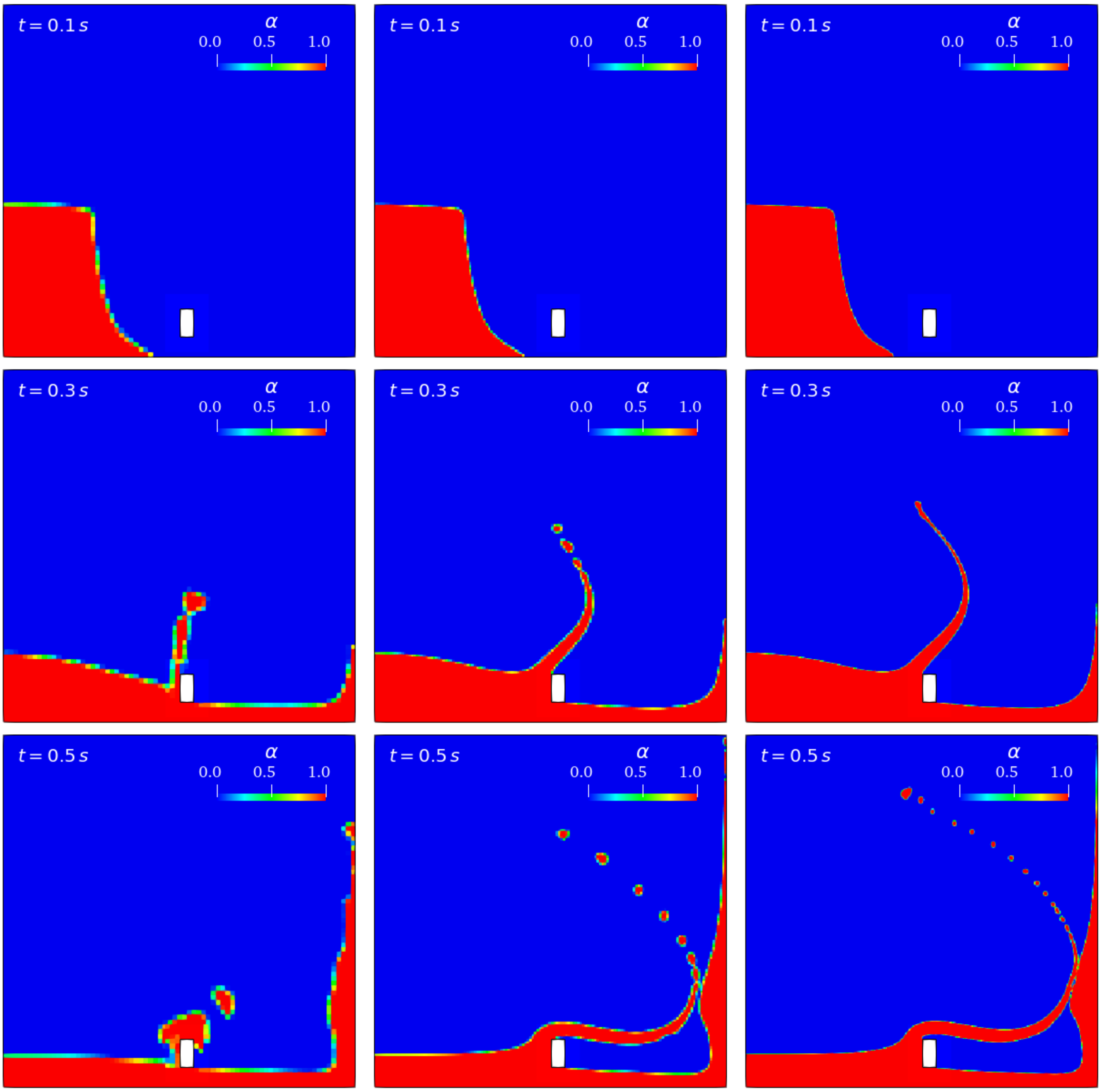

Figure 5: Fraction field distributions with different AMR levels at various time instants (*(left)* AMR = 0, *(mid.)* AMR = 1, *(right)* AMR = 2).

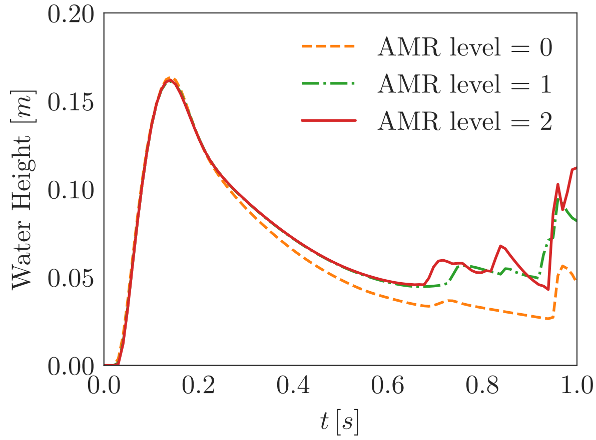

Figure 6: Time history of the vertical water heights.

The active cells in the background and body meshes are shown in Figure 7. The cells close to the interface have been refined properly, and the overset cell types have been detected correctly.

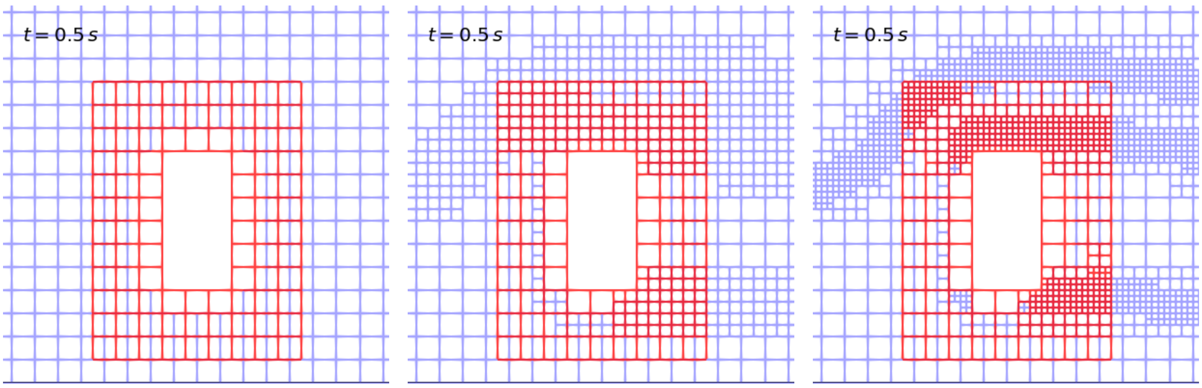

(a) AMR = 0 (b) AMR = 1 (c) AMR = 2

Figure 7: Active cells in the overset meshes at $t = 0.5\,s$.

3.2 3D Dam-breaking Simulation

The interface profiles (0.5-isosurface) with different AMR levels at various time instants are shown in Figure 8. Again, the interface has been better resolved with increasing AMR level. As shown in Figure 9, the transient water heights at the pre-defined probe converged as the AMR level increases.

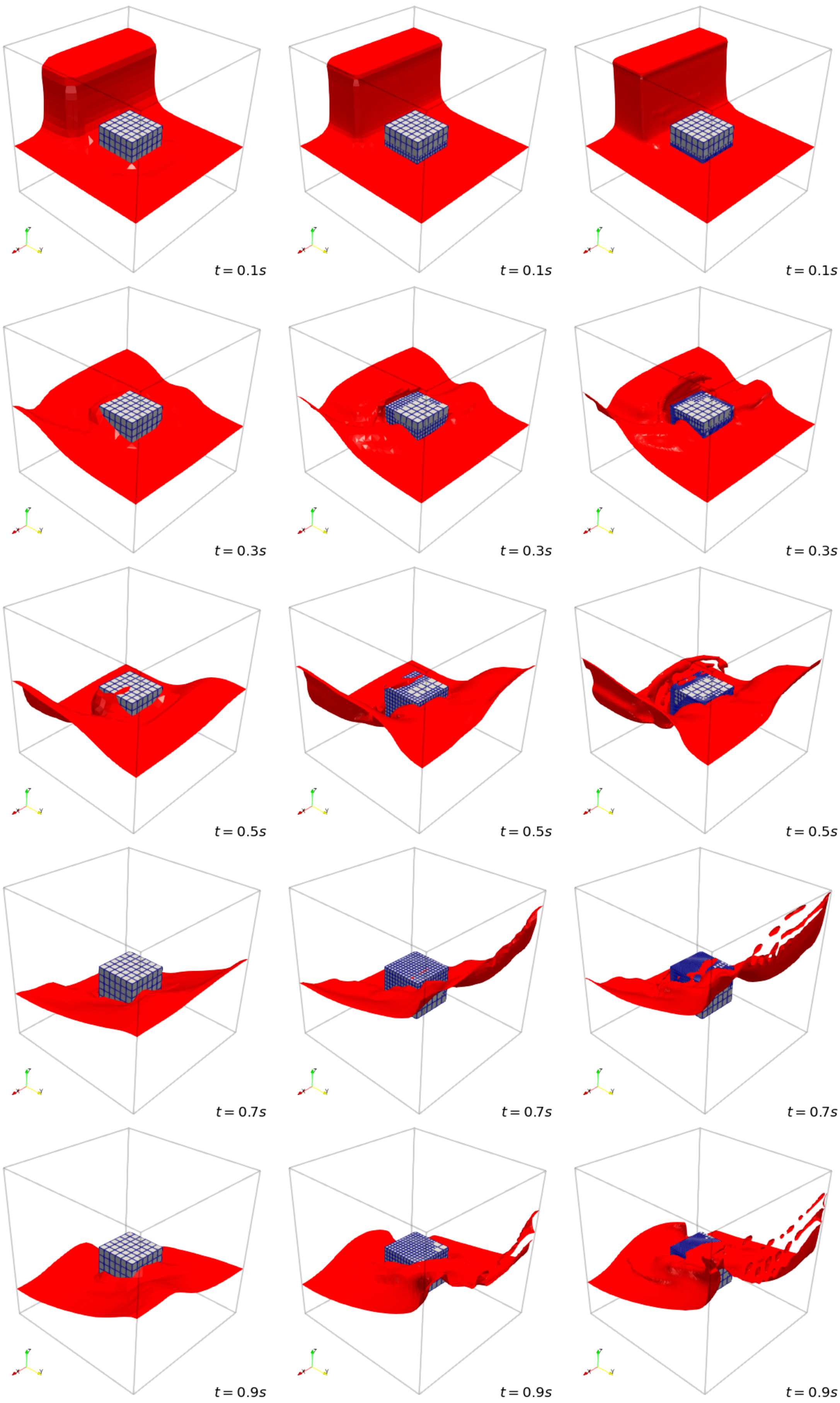

Figure 8: Interface profiles with different AMR levels at various time instants (*(left)* AMR $= 0$, *(mid.)* AMR $= 1$, *(right)* AMR $= 2$).

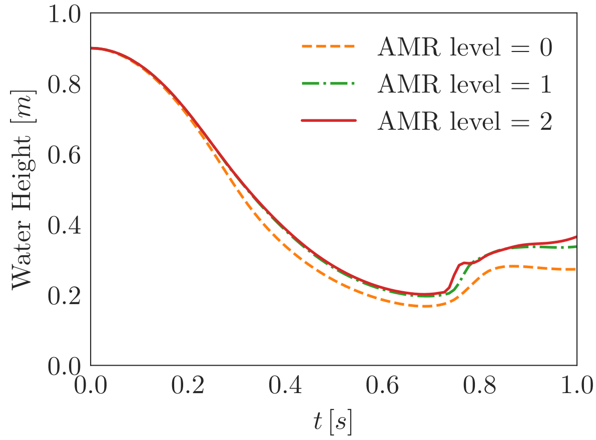

Figure 9: Time history of the vertical water heights.

The active cells in background and body meshes are shown in Figure 10. Again, the cells close to the interface have been refined properly, and the overset cell types have been detected correctly.

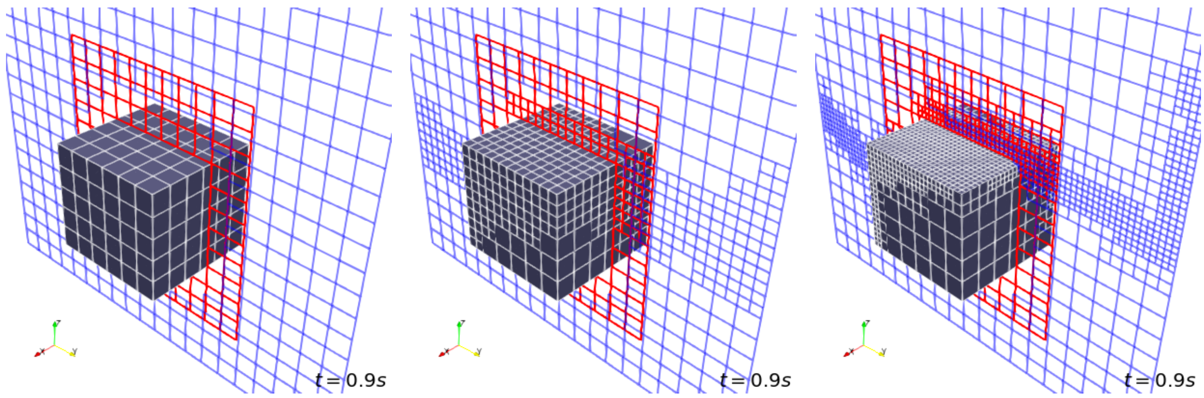

(a) AMR = 0 (b) AMR = 1 (c) AMR = 2

Figure 10: Active cells in the overset meshes at $t = 0.9\,s$.

4 CONCLUSIONS

An adaptive PLIC-VOF method with overset meshes has been introduced and tested by two dam-breaking problems. The computational domains are discretized by the overset meshes. The computational cells close to the interface regions are refined by the AMR method. The fraction field distributions and interface profiles with different refinement levels have been compared and found to be better resolved as the AMR level increased. The active cells in background and body meshes have been compared with increasing refinement levels and found to be appropriately refined and categorized.

ACKNOWLEDGEMENTS

This work was conducted at Argonne National Laboratory and supported by the U.S. Department of Energy, Office of Nuclear Energy, under Contract DE-AC02-06CH11357. The authors are thankful to all those involved in the organization of MARINE 2021, all the contributors that will enrich this event.

GOVERNMENT LICENSE

References

Yanni Chang, Dezhi Dai, and Albert Y Tong. A comparative study of interpolation schemes in overset meshes for the PLIC-VOF method in multiphase flows. In *ASME 2020 Fluids Engineering Division Summer Meeting collocated with the ASME 2020 Heat Transfer Summer Conference and the ASME 2020 18th International Conference on Nanochannels, Microchannels, and Minichannels*. American Society of Mechanical Engineers Digital Collection, 2020.

Dezhi Dai and Albert Y Tong. An analytical interface reconstruction algorithm in the PLIC-VOF method for 2D polygonal unstructured meshes. *International Journal for Numerical Methods in Fluids*, 88:265–276, 2018.

Dezhi Dai and Albert Y Tong. Analytical interface reconstruction algorithms in the PLIC-VOF method for 3D polyhedral unstructured meshes. *International Journal for Numerical Methods in Fluids*, 91:213–227, 2019.

Daniel Rettenmaier, Daniel Deising, Yun Ouedraogo, Erion Gjonaj, Herbert De Gersem, Dieter Bothe, Cameron Tropea, and Holger Marschall. Load balanced 2D and 3D adaptive mesh refinement in OpenFOAM. *SoftwareX*, 10:100317, 2019.

Johan Roenby, Henrik Bredmose, and Hrvoje Jasak. A computational method for sharp interface advection. *Royal Society Open Science*, 3(11), 2016. doi: 10.1098/rsos.160405.

Henning Scheufler. https://github.com/DLR-RY/VoFLibrary.

Henning Scheufler and Johan Roenby. Accurate and efficient surface reconstruction from volume fraction data on general meshes. *Journal of computational physics*, 383:1–23, 2019.